Available online at www.sciencedirect.com
SCIENCE DIRECT
Chemical Physics Letters 418 (2006) 549–554
CHEMICAL PHYSICS LETTERS
www.elsevier.com/locate/cplett

First-principles study of the stability and electronic properties of sheets and nanotubes of elemental boron

Kah Chun Lau [a], Ranjit Pati [a], Ravindra Pandey [a,*], Andrew C. Pineda [b,c]

[a] *Department of Physics and Multi-scale Technology Institute, Michigan Technological University, 1400 Townsend Drive, Houghton, MI 49931-1295, United States*
[b] *Department of Chemistry, University of New Mexico, Albuquerque, NM 87131-0001, United States*
[c] *US Air Force Research Laboratory, Kirtland Air Force Base, NM 87117, United States*

Received 29 July 2005; in final form 18 October 2005
Available online 1 December 2005

Abstract

The structural and electronic properties of sheets and nanotubes of boron are investigated using density functional theory. The calculations predict the stability of a novel reconstructed {1221} sheet over the 'idealized' triangular {1212} sheet. Nanotubes formed by wrapping the half-metallic {1221} sheet show a curvature-induced transition in their electronic properties. Analysis of the charge density reveals a mixed metallic- and covalent-type of bonding in the reconstructed {1221} sheet and the corresponding nanotubes, in contrast to metallic-type bonding in the idealized {1212} sheet and its analogous nanotubes.

Boron holds a unique place among the elements of the periodic table by having the most varied polymorphism, which includes quasicrystal [1] and novel nanostructures [2–6], in addition to the complex icosahedral networks observed in conventional boron-rich solids [7]. Based on a generalization of the Euler–Poincaré formula for a cylinder [8], it was suggested that boron nanotubes (BNTs) could be constructed by the appropriate 'wrapping' of an 'idealized' triangular boron sheet, referred to as the {1212} sheet. It is noteworthy to point out that the formation of the triangular boron sheet has not yet been verified by experiments. Analogous to the case of carbon nanotubes (CNTs), the wrapping in BNTs was described by a chiral vector $\mathbf{R} = n\mathbf{a} + m\mathbf{b}$, denoted as (n,m), where n and m are integers, and the BNTs were suggested to form 'zigzag', 'armchair' and 'chiral' structures depending upon the values of n and m [9]. A tubular structure consisting of the hexagonal pyramidal boron units was postulated [10], and non-self-consistent, non-orthogonal tight-binding (TB) calculations [11] were carried out on the nanotubular bundle structure which predicted the structure to be metallic. A new form of radially constricted bundles (ropes) have also been proposed [12], and pristine single wall 3 nm BNTs have been synthesized [4]. Most recently, a planar to tubular structural transition in the B_{20} cluster has been confirmed by photoelectron spectroscopy, suggesting that B_{20} may be considered as the basic building block for a boron tubular structure of diameter 0.52 nm [13].

Interestingly, the subtle questions about the stability and electronic properties of either the 'idealized' triangular boron sheet or the pristine, single-walled BNT have so far not been addressed. In this Letter, we propose to address these important questions using a *state-of-the-art* theoretical method based on periodic, gradient-corrected density functional theory. The calculated results show that the reconstructed {1221} sheet is more stable than the 'idealized' {1212} sheet. Surprisingly, in contrast to CNTs, the nanotubes formed by wrapping boron sheets are predicted to be energetically more favorable than their planar counterparts. The BNTs obtained by wrapping the {1221} sheet are found to be metallic showing a curvature-induced transition in their electronic properties. No curvature induced changes in electronic properties are found for the

* Corresponding author.
E-mail address: pandey@mtu.edu (R. Pandey).

0009-2614/$ - see front matter © 2005 Elsevier B.V. All rights reserved.
doi:10.1016/j.cplett.2005.10.104

case of the {1212} sheet. Furthermore, an analysis of the charge density reveals a prominent feature consisting of a mixed metallic- and covalent-type of bonding in the {1221} sheet and the corresponding nanotubes.

First-principles calculations were performed using the spin-polarized gradient-corrected density functional theory (DFT) with the Perdew–Wang (PW91) exchange and correlation functionals [14]. A plane wave basis set was used, and the valence–core interaction was described by the ultra-soft pseudopotential as implemented in the VIENNA AB INITIO SIMULATION PACKAGE (VASP) [15,16]. An energy cut-off of 208 eV in the plane wave expansion and of 443 eV for the augmented charge was used.

A supercell was constructed in which a BNT was placed in a rectangular grid. The wall to wall distance between the nanotubes was ~15 Å ensuring negligible interaction between the tube and its images, in contrast to the very small (~1.8 Å) inter-tubular spacing considered in previous studies [11]. The infinite open-end BNT is then built by stacking up the supercell in the z-direction, and the repeated basic unit is arranged at the centre of the xy-plane. For the single-layer boron sheet, we constructed a supercell by placing a part of the infinite boron sheet inside a rectangular grid with a surface-to-surface separation of ~10 Å. Calculations were deemed converged when changes in total energy were less than 10^{-5} eV and those in the inter-atomic forces were less than 0.01 eV/Å.

Boron sheet: we begin by considering four possible configurations for the boron sheet. As shown in Fig. 1, the 'idealized' {1212} configuration consists of a 'triangular' three-atom unit uniformly repeated in the y-direction in which each atom has the same number of nearest-neighbors. In the $\{1212\}^{b}$ configuration, the {1212} monolayer is buckled with a small atomic displacement of 0.2 Å in the alternate chains. On the other hand, the pair-buckled $\{1212\}^{pb}$ configuration consists of a sheet which is 'buckled' in the alternate pair chains. Lastly, we consider a reconstructed {1221} configuration with inversion symmetry in the unit cell. It can be considered as a 'triangular-square-triangular' unit network repeated in the y-direction.

The DFT calculations show the reconstructed {1221} configuration to be the most stable configuration: it is stable by 0.23 eV/atom relative to the idealized {1212} configuration. Both the $\{1212\}^{b}$ and $\{1212\}^{pb}$ configurations tend to converge to the idealized {1212} configuration when relaxed during the geometry optimization. The results are,

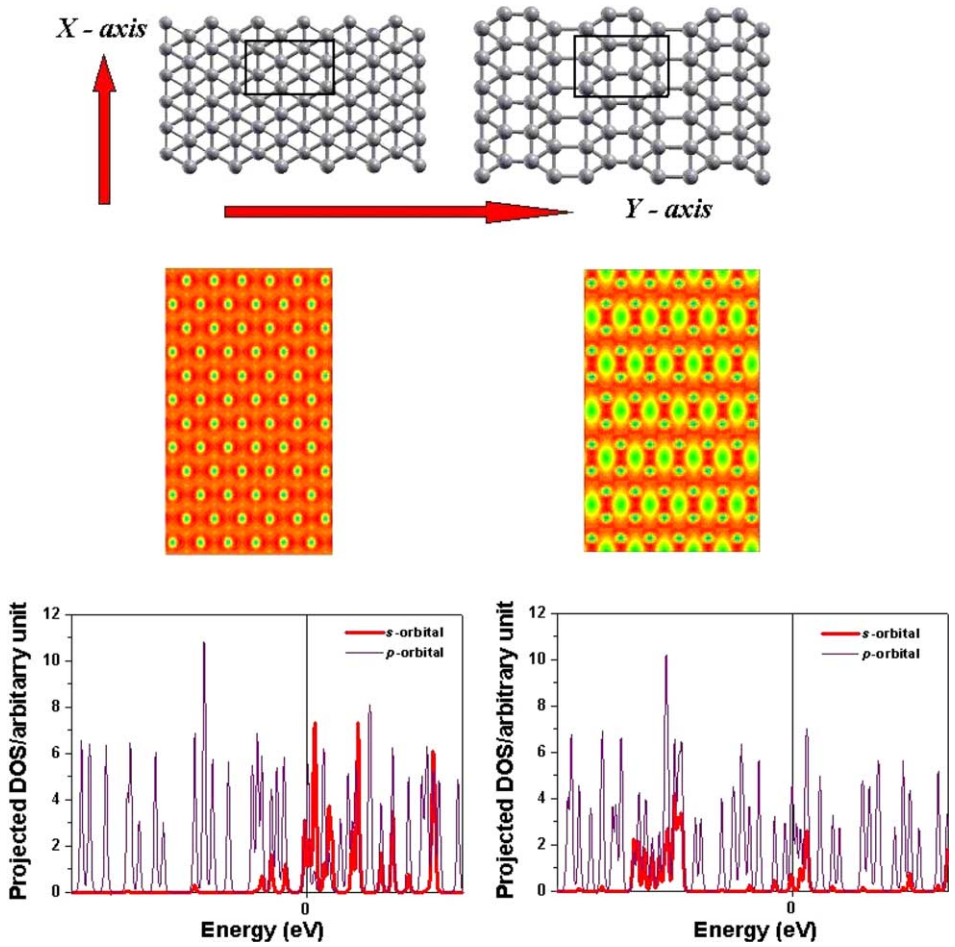

Fig. 1. (Top) Idealized {1212} sheet, and the reconstructed {1221} sheet. (Center) Total charge density of the {1212} and {1221} sheets. (Bottom) Projected density of states of the {1212} and {1221} sheets. The Fermi level is taken to be zero.

therefore, not in agreement with the previously reported cluster calculations, based on an ab initio plane wave approach, which found the 'buckled' configuration to be stable with respect to the 'unbuckled' configuration by 0.03 eV/atom [11].

The bonding in the idealized {1212} sheet is found to be dominated by out-of-plane π-type interactions resulting in delocalized charge density. We note that the idealized sheet consists of six coordinated boron atoms. However, this is not the case for the reconstructed {1221} sheet which shows anisotropic chemical bonding. Here, the coordination index of the boron atoms is five in the 'triangular-square-triangular' network, and in-plane σ-type interactions contribute significantly to the bonding. This results in a contraction of about 9% in R_{B-B} (Table 1). Analysis of the charge density, shown in Fig. 1, reveals that charge transfer between the delocalized multi-center triangular networks is saturated by the formation of directional covalent bonds that interconnect these triangular units. Fig. 1 also shows the projected density of states of both sheets. Note that the occupied states in the idealized {1212} sheet are dominated by contributions from p orbitals, whereas contributions from s orbitals become significant for the reconstructed {1221} sheet, resulting in a mixture of strong covalent and weak metallic-type bonding in {1221}. In this context, it is worth pointing out that the 2D sheets share some similarities in electronic properties with their fragments, namely, the planar boron clusters [6,17]. The dominant feature of out-of-plane π-type bonding interactions resulting in delocalized charge density in the idealized {1212} sheet can be attributed to the delocalized nature of the π-electrons in the planar boron clusters, which renders aromaticity and antiaromaticity to the corresponding clusters in analogy to bonding in planar hydrocarbons [6,17].

The uniform delocalized charge density found in the {1212} sheet yields isotropic features of metallic-like character in the band dispersion along the K_X and K_Y directions. Whereas the anisotropic nature of the chemical bonding in the {1221} sheet yields different dispersion along K_X and K_Y, thereby leading to direction-dependent electronic properties (Fig. 2). The directional σ-type bonding opens up the gap in the band structure along K_Y by lifting the degeneracy of the bands. In contrast, due to the delocalized π-type bonding in the X-direction, almost no gap appears along K_X with the uppermost valence band crossing the Fermi level. The calculated band gap at Γ along K_Y for the {1221} sheet is ~0.45 eV, which is smaller than the calculated indirect band gap of 1.72 eV found in crystalline α-B_{12} [17]. The idealized {1212} sheet is predicted to be metallic with finite density of states at the Fermi energy.

Boron nanotube: we now focus on BNTs obtained by folding the more stable reconstructed {1221} sheet. Following the well-established conventions proposed for the carbon nanotubes [9], we consider the $(n,0)$ zigzag (i.e. type-I) and $(0,m)$ armchair (i.e. type-II) nanotubes of the elemental boron with $n,m = 6$ and 12, respectively (Fig. 3). The results for the $(n,0)$ zigzag (i.e. type-III) BNT formed by wrapping the idealized {1212} boron sheet are also presented. We note that the optimized structures of the sheets and nanotubes of boron are predicted to be non-magnetic.

In general, the calculated bond lengths of all BNTs are comparable to the intra-icosahedral and inter-icosahedral bond lengths of the conventional α-B_{12} and β-B_{108} phases of the bulk boron [18,19]. As compared to the corresponding reconstructed {1221} sheets, the changes in bond lengths for the optimized structures in type-I and type-II BNTs are found within a range of 7% (Table 1), with R_{B-B} of the shortest directional bond remaining nearly the same. The cohesive (or binding) energy of a BNT is defined as $E_c(\mathrm{BNT}) = E_T(\mathrm{B}) - E_T(\mathrm{BNT})/N$, where the energy of the B atom is $E_T(\mathrm{B})$, and the total energy per atom of a BNT consisting of N atoms in the supercell is $E_T(\mathrm{BNT})/N$. Accordingly, $E_c > 0$ indicates a stable configuration on the Bohr–Oppenheimer energy surface. The E_c values are comparable to the cohesive energy of 5.81–6.95 eV of the α-B_{12} and β-B_{108} phases of the bulk boron [7,18–20].

Among the nanotubes considered, the (6,0) zigzag type-I is found to be more stable than the (0,6) armchair type-II and (6,0) zigzag type-III by 0.26 and 0.47 eV/atom, respectively. Two degenerate radially constricted configurations

Table 1
Structures and energetics of sheets and nanotubes of elemental boron

System		Symmetry	N (atoms/supercell)	Diameter (Å)	R^{intra}_{B-B} (Å)	E_{coh} (eV/atom)	E_{strain} (eV/atom)
Sheet	{1221} sheet	C_{2h}	8	–	1.69–1.85	5.64	0.00
	{1212} sheet	C_{2v}	8	–	1.85	5.41	0.00
Nanotube zigzag type-I	(6,0)	D_{2h}	24	3.86	1.69-1.99	5.80	−0.16
	(12,0)	D_{4h}	48	7.69	1.70–1.99	5.75	−0.11
Armchair type-II	$(0,6)^r$	C_{1h}	24	6.13	1.63–1.85	5.54	0.10
	$(0,6)^h$	C_{1h}	24	5.89	1.64–1.85	5.53	0.11
	$(0,12)^f$	C_{1h}	48	11.51	1.68–1.88	5.66	−0.02
Zigzag type-III	(6,0)	D_{2d}	24	3.85	1.70–2.00	5.33	0.08
	(12,0)	D_{4h}	48	6.63	1.66–1.82	5.43	−0.02

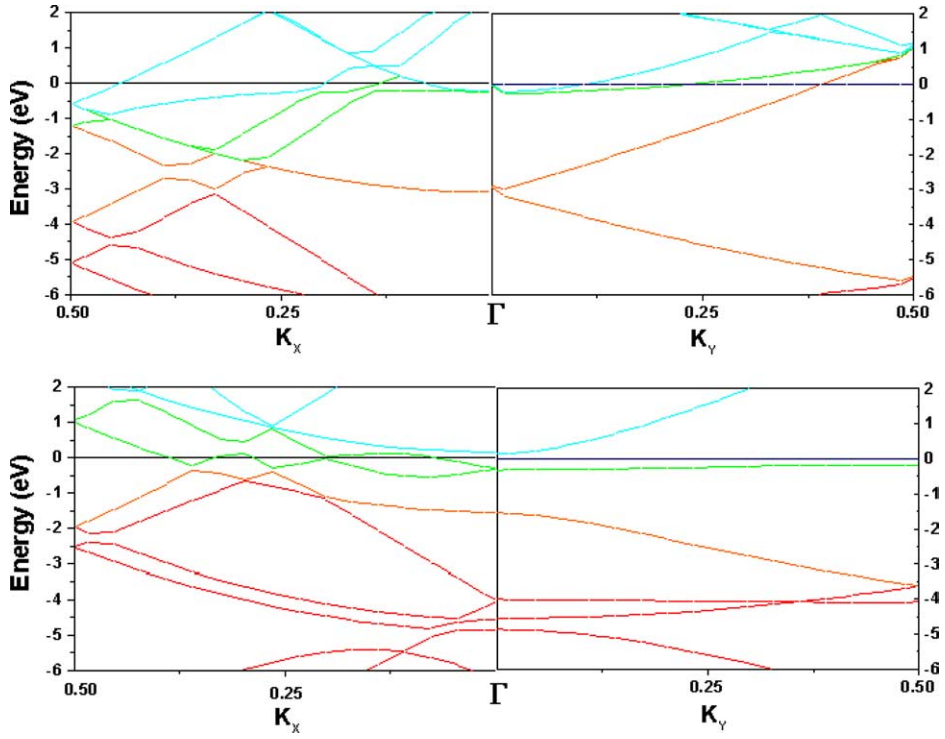

Fig. 2. Band structure along K_X and K_Y. (Top) {1212} sheet, (Bottom) {1221} sheet. The Fermi level is taken to be zero.

are predicted for the armchair type-II, namely '*rhombus*' $(0,6)^{r}$ *and* '*hexagonal*' $(0,6)^{h}$-like cylinders. We note here, that the folding of the {1221} sheet into the (0,6) armchair introduces a large strain in the strong directional covalent bonding. During the geometry optimization, this strain is relieved by the significant buckling of its surface together with radial distortions. The order of stability of BNTs remains the same as their diameter is increased. The (12,0) zigzag type-I is stable by 0.09 and 0.32 eV/atom relative to the (0,12) armchair type-II and (12,0) zigzag type-III, respectively.

By convention, the strain (or curvature) energy is the energy required to form a tubular structure by folding the boron sheet, and is defined as $E_s(\mathrm{BNT}) = E_c(\mathrm{sheet}) - E_c(\mathrm{BNT})$. The calculated results summarized in Table 1 suggest that the zigzag BNTs are energetically more favorable than the corresponding sheets, unlike the case of carbon where the graphene sheet is energetically favored over the CNT [21]. For example, the strain energy of the (6,0) zigzag type-I BNT of ~4 Å diameter formed by wrapping the reconstructed {1221} sheet, is found to be −0.16 eV/atom. At the same level of theory, the E_s of the (5,0) zigzag CNT of ~4 Å diameter is ~0.50 eV/atom [21]. In CNTs, the strain energy, which is insensitive to the chirality of the tube, shows a small variation with the diameter of the tube [9,22]. On the other hand, the mixture of strong two-center, directional covalent (σ-type) bonds along the tube axis and multi-center metallic-like (π-type) bonds along the circumference of the tube stabilizes the zigzag type I BNT over the sheet resulting in a negative value in the strain energy.

For the case of the (6,0) zigzag type-III of ~4 Å diameter, the sheet is slightly more stable (~0.1 eV/atom). The stability of the sheet relative to the BNT, however, decreases with increasing diameter making the BNTs more stable at ~8 Å diameter. This is in contrast to what was predicted for the zigzag type-I whose stability decreases with increasing diameter of the nanotube. The difference in stability can be attributed to the dominance of π-type interactions in the zigzag type-III tubes. Despite having a larger diameter than the zigzag type-I, the (0,6) armchair type-II of ~6 Å diameter is ~0.1 eV/atom less stable than the {1221} sheet. In this respect, the strain energy due to the folding of the {1221} sheet into the (0,6) armchair BNT, is caused by directional σ-type covalent bonding.

Fig. 4 shows the band structure of the zigzag type-III BNTs where the bands are mostly derived from boron $p_{x,y}$ and p_z states. The partially filled bands having $p_{x,y}$-character are associated with top of the valence band, and are responsible for the metallic character of the nanotube. It is followed by the valence band of p_z-character which is highly dispersive at about 2.5 eV below E_F level. In nanotubes, the curvature-induced effect shifts the lowest conduction band downward, facilitating a larger overlap with the uppermost valence band, which increases the metallic character of the nanotube. This type of metallic feature in the idealized {1212} sheet and type-III BNT has also been observed in the analysis of density of states (DOS), which indicates a finite DOS at the Fermi energy.

For the zigzag (6,0) type-I BNT, the band structure calculated along the tube axis, K_Z is shown in Fig. 4. The

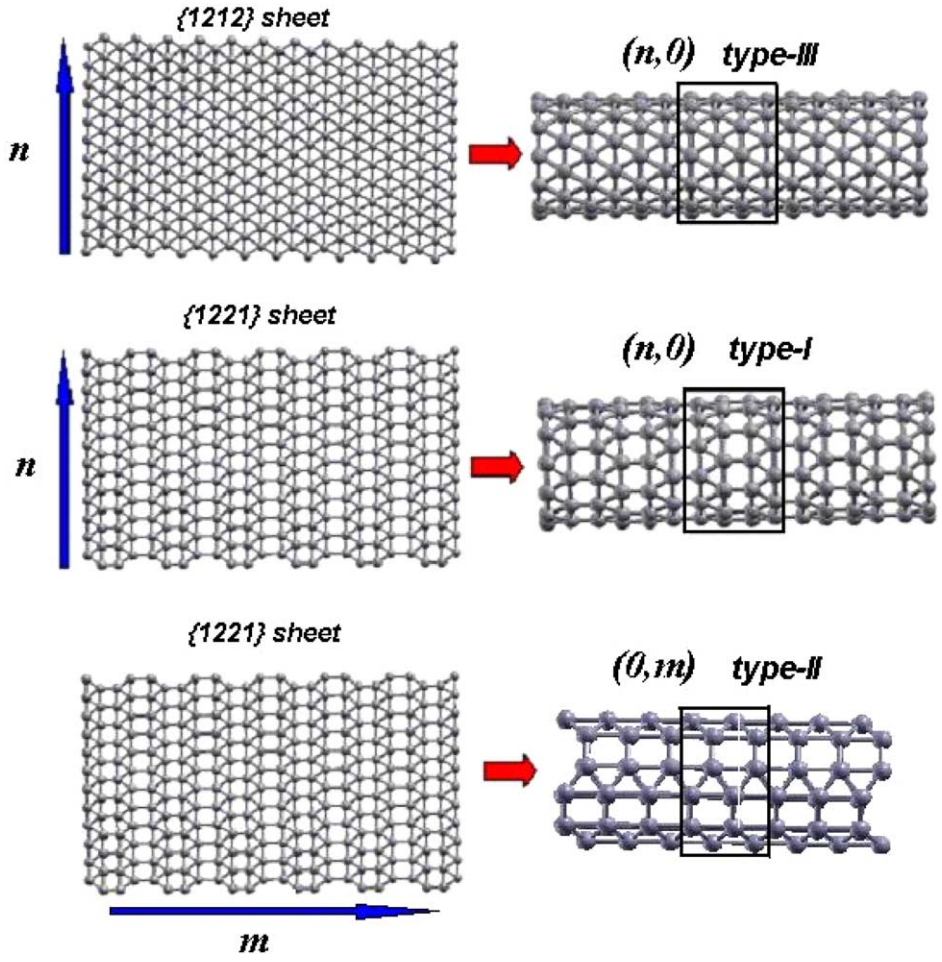

Fig. 3. Sheet configurations forming nanotubes with chiral vector (blue arrow) $\boldsymbol{R} = n\mathbf{a} + m\mathbf{b}$, where n and m are integers: (Top) $(n,0)$ zigzag type-III. (Center) $(n,0)$ zigzag type-I. (Bottom) armchair $(0,m)$ type-II. (For interpretation of the references in colour in this figure legend, the reader is referred to the Web version of this article.)

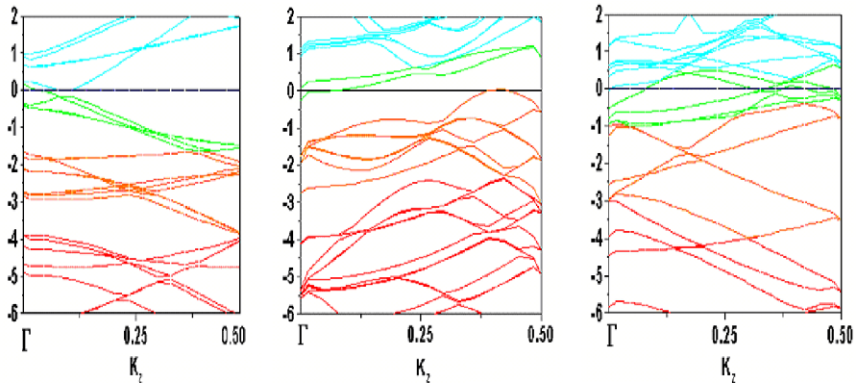

Fig. 4. Band structure along the tube axis, K_Z. (Left) – (6,0) type-I. (Center) – (0,6) type-II. (Right) – (6,0) type-III. The Fermi level is taken to be zero.

uppermost valence band does not cross the Fermi energy, but the lowest conduction band crosses the Fermi energy near Γ to close the gap. A nearly zero gap is also predicted for the (12,0) BNT. Thus, a curvature-induced transition from anisotropic to isotropic behavior in the electronic properties is predicted for BNTs constructed by wrapping the reconstructed {1221} sheets. Analysis of the charge density further suggests the presence of mixed delocalized multi-center and the directional covalent bonds in BNTs, as also found in the {1221} sheet. The calculated DOS for the type-I BNT shows no gap with a finite DOS at the Fermi energy confirming its metallic properties. It is essential to point out that the curvature-induced transition in the electronic properties of type-I BNTs is rather similar

to the curvature-induced metallicity due to the σ and π^* *hybridization* [21,23] found in small diameter $(n,0)$ 'zigzag' CNTs (with $n = 4$, 5 and 6). Likewise, the $(0,m)$ armchair type-II BNTs with $m = 6$, 12 are predicted to be metallic (Fig. 4). It has previously been pointed out that the emergence of tubular elemental boron clusters (e.g. B_{20} [13]) which mark the 2D-to-3D structural transition in elemental boron clusters suggests that formation of boron nanotubes is feasible. The most stable configuration of B_{20} (i.e. a double-ring BNT fragment) with diameter ~0.52 nm, can be found in (10,0) zigzag BNT, which is constructed from either the {1221} or the {1212} boron sheet. On the other hand, the basic unit of the most stable (6,0) zigzag type-I BNT considered in this study, with diameter ~0.40 nm, can be found in B_{24} [5].

In summary, periodic density functional theory was used to study the stability, morphology and electronic properties of boron sheets and nanotubes. We predict the stability of a novel reconstructed {1221} boron sheet over the idealized {1212} sheet. The presence of the directional σ-type interactions with the delocalized π-type interactions appears to stabilize the reconstructed {1221} sheet. Such mixed bonding interactions also yield anisotropy in the electronic properties with a direct band gap of 0.45 eV in the K_Y direction and no gap in K_X direction. However, BNTs formed by wrapping the reconstructed sheet are predicted to be metallic due to a curvature-induced transition in the electronic properties. Furthermore, the calculations predict that the zigzag type-I BNT formed by wrapping the reconstructed {1221} sheet to be more stable than the sheet itself.

Acknowledgments

We thank Dilip Kanhere, Mrinalini Deshpande, Aurora Costales and Miguel Blanco for helpful discussions during this work. This work was partially supported by DARPA through ARL Contract No. DAAD17-03-C-0115. We also gratefully acknowledge CSERC MTU for access to their computing facility.

References

[1] M. Takeda, K. Kimura, A. Hori, H. Yamashita, H. Ino, Phys. Rev. B 48 (1993) 13159.
[2] C.J. Otten, O.R. Lourie, M. Yu, J.M. Cowley, M.J. Dyer, R.S. Ruoff, W.E. Buhro, J. Am. Chem. Soc. 24 (2001) 4564.
[3] T.T. Xu, J. Zheng, N. Wu, A.W. Nicholls, J.R. Roth, D.A. Dikin, R.S. Ruoff, NanoLetters 4 (2004) 963.
[4] D. Ciuparu, R.F. Klie, Y. Zhu, L. Pfefferle, J. Phys. Chem. B 108 (2004) 3967.
[5] K.C. Lau, M.D. Deshpande, R. Pati, R. Pandey, Int. J. Quantum Chem. 103 (2005) 866.
[6] H. Zhai, B. Kiran, J. Li, L.S. Wang, Nat. Mater. 2 (2003) 827.
[7] E.L. Muetterties (Ed.), The Chemistry of Boron and its Compounds, John Wiley, New York, 1967.
[8] A. Gindulytė, W.N. Lipscomb, L. Massa, Inorg. Chem. 37 (1998) 6544.
[9] R. Saito, G. Dresselhaus, M.S. Dresselhaus, Physical Properties of Carbon Nanotubes, Imperial College Press, London, 2003.
[10] I. Boustani, Phys. Rev. B 55 (1997) 16426.
[11] I. Boustani, A. Quandt, E. Hernandez, A. Rubio, J. Chem. Phys. 110 (1999) 3176.
[12] J. Kunstmann, A. Quandt, Chem. Phys. Lett. 402 (2005) 21.
[13] B. Kiran, S. Bulusu, H. Zhai, S. Yoo, X. Zeng, L.S. Wang, Proc. Natl. Acad. Sci. USA 102 (2005) 961.
[14] J.P. Perdew, Y. Wang, Phys. Rev. B 45 (1992) 13244.
[15] G. Kresse, VASP (VIENNA AB INITIO SIMULATION PACKAGE) software J. Hafner, Phys. Rev. B 47 (1993) 558.
[16] G. Kresse, J. Furthmuller, Phys. Rev. B 54 (1996) 11169.
[17] H. Zhai, A.N. Alexandrova, K.A. Birch, A.I. Boldyrev, L.S. Wang, Angew. Chem., Int. Ed. 42 (2003) 6004.
[18] J. Zhao, J.P. Lu, Phys. Rev. B 66 (2002) 092101.
[19] N. Vast, S. Baroni, G. Zerah, J.M. Besson, A. Polian, M. Grimsditch, J.C. Chervin, Phys. Rev. Lett. 78 (1997) 693.
[20] D.R. Lide, CRC Handbook of Chemistry and Physics, CRC Press, Boca Raton, 1995.
[21] O. Gülseren, T. Yildirim, S. Ciraci, Phys. Rev. B 65 (2002) 153405.
[22] D.H. Robertson, D.W. Brenner, J.W. Mintmire, Phys. Rev. B 45 (1992) 12592.
[23] X. Blasé, L.X. Benedict, E.L. Shirley, S.G. Louie, Phys. Rev. Lett. 72 (1994) 1878.